

# Phase slip phenomena in superconductors: from ordered to chaotic dynamics

Mathieu Lu-Dac and V. V. Kabanov  
*Jozef Stefan Institute, Jamova 39, 1001 Ljubljana, Slovenia*

We consider flux penetration to a 2D superconducting cylinder. We show that in the low field limit the kinetics is deterministic. In the strong field limit the dynamics becomes stochastic. Surprisingly the inhomogeneity in the cylinder reduces the level of stochasticity because of the predominance of Kelvin-Helmholtz vortices.

PACS numbers: 74.40.Gh, 74.81.-g, 74.78.Na, 74.40.De

The kinetics of vortex production in superconductors and superfluids is one of the intriguing problems of condensed matter physics. It is interesting not only in the field of solid state physics but represents as well a very good model to study topological phase transitions in cosmology and other branches of physics [1]. In the last few decades different scenarios for vortex production in superconductors and superfluids were proposed. The most common way to produce vortices is to increase the superfluid velocity in order to reduce the energy barrier between homogeneous flow and flow with vortices. This mechanism is observed in rotating  $^3\text{He}$  where vortex nucleation and critical velocities are measured [3]. In 2D homogeneous superconducting films, increasing the current leads to dynamics which are similar to the phase slip (PS) transition in 1D [4]. The order parameter (OP) reaches zero along a straight line across the film and the phase displays a  $2\pi$  jump along this line. This PS line solution [5] corresponds to the deterministic and most ordered PS kinetics in 2D. The inhomogeneity caused by current contacts leads to a qualitatively similar picture. The OP is strongly suppressed along a straight line across the film but it reaches zero only at two points on this line. This pair of vortices is called kinematic vortex-antivortex (VaV) pair [6]. It spreads quickly in opposite directions along this line propagating the  $2\pi$  jump of the phase. Therefore PS occurs without formation of well defined VaV pairs [7].

A different scenario of vortex production was proposed by Kibble[8] and Zurek[9] (KZ). When the sample is quickly quenched through the critical temperature  $T_c$ , the nucleation of the low temperature phase starts in different places with uncorrelated phases of OP. Then, domains grow and start to overlap leading to the formation of vortices. This mechanism is a promising way to test cosmological theories in condensed matter physics [10, 11]. This dynamics is stochastic and sensitive to small variations of initial conditions. On the other hand the dependence of the vortex density on the quench time and their spatial correlation are universal. Later, in Refs. [12, 13], it was proposed that the quench occurs not only due to fast temperature change but also due to the temperature front propagation. Aranson *et al.* considered the case of a temperature quench in the presence of ex-

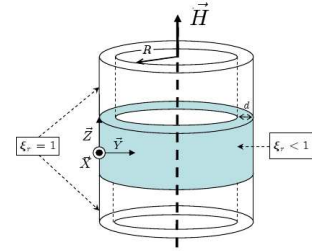


FIG. 1: Geometry of the system : a 2D cylinder with an applied magnetic field  $\mathbf{H}$ .

ternal current [14]. The new phase with zero current grows after the quench. Therefore on the border of the quenched region, the superfluid velocity has tangential discontinuity, leading to vortex formation, similarly to the classical hydrodynamic Kelvin-Helmholtz (KH) instability [15] which is also known in superfluids [16, 17]. Moreover, the KH instability suppresses the development of KZ vortices [14]. In this paper, kinematic VaV, KZ and KH vortices are distinguished by their production mechanism although they are topologically equivalent.

To demonstrate how deterministic type of dynamics becomes stochastic, we model a superconducting film rolled on a cylinder in an external time dependent magnetic field parallel to the cylinder axis (Fig.1). Depending on the applied magnetic field and the dimensions of the ring, we follow the evolution from the deterministic PS line dynamics to the stochastic behavior described by the KZ mechanism. In the proposed model, topological defects are generated by the intrinsic quench induced by the external field. The evolution towards stochastic behavior is strongly influenced by the KH instability which develops in the presence of inhomogeneities. To model the inhomogeneity of the film we assume that there is a thin stripe of superconductor along the film with a different coherence length. The thickness of the film  $d$  is small  $d \ll \xi \ll \lambda_{\text{eff}}$ . Here  $\xi$  is the coherence length and  $\lambda_{\text{eff}}$  is the Pearl penetration depth. Therefore we can neglect all corrections to the external magnetic field  $\mathbf{H}$  caused by the current in the film. The radius of the film is  $R > \xi$ . The time dependent Ginzburg-Landau (TDGL) equation

in dimensionless units has the form:

$$u\left(\frac{\partial\psi}{\partial t} + i\Phi\psi\right) = b(z)(\psi - \psi|\psi|^2) - (i\nabla + \mathbf{a})^2\psi + \eta. \quad (1)$$

Here  $\psi$  is the dimensionless complex OP, the spacial coordinate  $\mathbf{r}$  is measured in units of  $\xi$  and time is measured in units of phase relaxation time  $\tau_\theta = \frac{4\pi\lambda_{\text{eff}}\sigma_n}{c^2}$ ,  $\lambda_{\text{eff}} = \frac{\lambda^2}{d}$ ,  $\lambda$  is the bulk penetration depth,  $\sigma_n$  is the normal state conductivity, and  $c$  is the speed of light. The parameter  $u = \frac{\tau_\psi}{\tau_\theta}$  is a material dependent parameter, where  $\tau_\psi$  is the relaxation time of the amplitude of the OP. According to the microscopic theory,  $u$  is ranging from 5 to 12 but we assume  $0 < u < \infty$ . The vector potential  $\mathbf{a}$  is measured in units of  $\frac{\phi_0}{2\pi\xi}$  where  $\phi_0$  is the flux quantum. The function  $b(z)$  models the  $z$  dependence of the coherence length  $\xi(z)$ . As shown in Fig.1, we chose  $\xi(z) = \xi/\sqrt{b(z)}$  and  $b(z) = 1 - b^2\vartheta(z - w/4)\vartheta(3w/4 - z)$ . Here  $w$  is the width of the film in units of  $\xi$ ,  $b$  parameterizes the level of inhomogeneity of the film and  $\vartheta(x)$  is the Heaviside step function. Here we use periodic boundary conditions and the boundary condition with vacuum [18] at  $z = 0$  and  $z = w$ . The equation for the electrostatic potential  $\Phi$ , measured in units of  $\frac{\phi_0}{2\pi c\tau_\theta}$ , where  $e$  is the electronic charge and  $\hbar$  is the Planck constant, reads:

$$\nabla^2\Phi = -\nabla\left[\frac{i}{2}(\psi^*\nabla\psi - \psi\nabla\psi^*) + \mathbf{a}|\psi|^2\right]. \quad (2)$$

To model the process of vortex formation we assume that at time  $t < 0$  external magnetic field is absent. At  $t = 0$  the field suddenly appears and stays constant for  $t > 0$  i.e. tangential component of the vector potential is  $a\vartheta(t)$ . We thus study the kinetics of the vortex generation as a function of  $a$  with different values of  $u$ .

Let us first consider the stability of the solution in the uniform case. We linearize the TDGL Eqs.(1,2) in small fluctuations of OP  $f(\mathbf{r}, t) = \psi(\mathbf{r}, t) - \psi_0$  and search for a solution in the form  $f(\mathbf{r}, t) = \sum_{\mathbf{k}} C_{\mathbf{k}} \exp(i\mathbf{k}\mathbf{r} + \lambda_{\mathbf{k}}t)$ . It is clear that the transverse  $k_z$  component always contributes to the stability of the initial state. Therefore, the condition  $\lambda_{\mathbf{k}} > 0$  is the same as in 1D [4]:  $\frac{\phi}{\phi_0} \gg \frac{R}{\xi\sqrt{3}}$ , where  $\phi$  is the magnetic flux through the ring at  $t > 0$ . This condition provides a rough estimate for the number of the expected PS events  $N \sim \frac{\phi}{\phi_0}$ . It defines the first critical value of the external field  $a_{c1} = 1/\sqrt{3}$ . Therefore, in the low field limit  $a_{c1} \leq a \leq 1$ , the dynamics will be similar to the 1D case with very weak  $z$ -dependence. Well defined vortices may appear in this region of the field if the film is inhomogeneous as shown in Fig.1. The situation is different when the field  $a$  increases further. Dropping  $k_z = 0$ , the eigenvalues are:

$$\lambda_{\mathbf{k}}^{(1,2)} = -\psi_0^2/2 + (1 - 2\psi_0^2 - a^2 - k^2)/u \pm \sqrt{(16\psi_0^2a^2 + \psi_0^4(u-2)^2 + 16k^2a^2)/4u^2} \quad (3)$$

$\lambda_{\mathbf{k}=0} = \frac{1-2\psi_0^2-a^2}{u} - \frac{\psi_0^2}{2} - \sqrt{(16\psi_0^2a^2 + \psi_0^4(u-2)^2)/4u^2}$  describes the decay rate of the uniform solution. On

the other hand for finite  $k$ ,  $\lambda_{\mathbf{k}}$  is positive and characterizes the growth of the corresponding Fourier components  $C_{\mathbf{k}}$ . The fastest growth is found for  $k = \frac{1}{4a}\sqrt{-16u\psi_0^2a^2 - \psi_0^4(u-2)^2 + 16a^4}$  and the rate is determined by  $\lambda_{\text{max}} = \frac{1}{16ua^2}(8(u-4)\psi_0^2a^2 + 16a^2 + \psi_0^4(u-2)^2)$ . The qualitative difference in kinetics takes place when the decay rate of the uniform solution becomes faster than the growth of the new phase. This effect is similar to the quench through  $T_c$  in the KZ mechanism [1, 8]. We find that at  $a > a_{c2} = \sqrt{2}$ , the OP is suppressed to zero and the growth of the phase with finite  $k$  is accompanied by the rapid development of vortices. The density of vortices may be estimated using Zurek arguments where the quench time should be replaced by  $\tau_Q = (a^2 - 1)^{-1}$  leading to  $n \propto \tau_Q^{-1/2}$  [19].

We simulate Eqs.(1,2) using the fourth order Runge-Kutta method. The spatial derivatives are evaluated using a finite difference scheme of second order or using a fast fourier transform algorithm depending on the boundary conditions. The choice of the algorithm is made to optimize the convergence and the calculation times. The calculations are performed for the vector potential  $0 < a < 5$  and for the total flux  $\phi$  through the ring ranging from 0 to  $50\phi_0$ .

We investigate the flux penetration into the homogeneous ring for two different boundary conditions. In the case of periodic boundary conditions we identify different regimes in accordance with Eq.(3). In the small field limit  $a < a_{c1}$  the ring is in a stable state and the penetration of the magnetic flux into the ring can only be induced by a very strong noise  $\eta$  in Eq.(1). When  $a_{c1} < a < a_{c2}$ , in agreement with the stability analysis, the PS kinetics depends on the external magnetic field. When  $\frac{\phi}{\phi_0} < 10$  the kinetics is similar to the 1D case. The transition is characterized by one or more lines in the  $z$ -direction where the OP decreases to zero (the PS line case [6]). These lines may appear simultaneously or consecutively in time, depending on  $u$  [4]. As expected, the number of PS events is determined by the ratio  $\frac{\phi}{\phi_0}$ . These PS lines represent the limiting case of kinematic VaV pairs travelling with infinite velocity.

When the flux is increased ( $\frac{\phi}{\phi_0} > 10$ ), the kinematic vortices become clearly distinguishable. In Fig.2(a), we present the time evolution of the average value of the OP together with the time dependence of the number of vortices in the sample. The kinetics is characterized by series of consecutive PS events well separated in time (Fig.2(a)). As it was noticed [20], few VaV pairs may propagate along the same line at the same time. PS events are produced by kinematic VaV pairs propagating along the same line where the amplitude of OP is reduced. Kinematic vortices can propagate in the same direction, one after another or in opposite direction leading to annihilation of VaV pairs and accelerating the dynamics. Contrary to [7], kinematic VaV pairs are formed

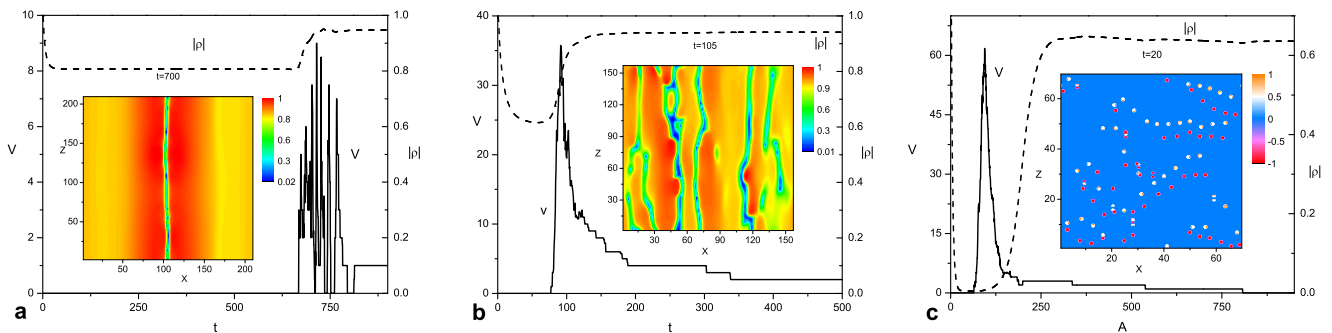


FIG. 2: (Color online) Total number of vortices  $v$  in the system and the sample average value  $|\rho|$  of the OP as a function of time for  $\phi/\phi_0 = 20$  and  $a = 0.6$  (a),  $a = 0.8$ (b) and  $a = 1.8$  (c). The insets represent snapshots the amplitude of OP at  $t = 700$  (a) and  $t = 105$  (b). For the quenched case (c), the snapshot displays the local vorticity at  $t = 20$ .

without any inhomogeneity in the film. At higher fluxes kinematic VaV pairs are randomly created on the line like in the case of a "1D quench". In the  $x$  direction, the dynamics remains very ordered with values of the standard deviation of the position of the vortices  $\sqrt{\delta x^2}$  approaching  $0.5\xi$ .

With the further increase of  $a$  the number of PS lines increases and the kinetics becomes more stochastic because of the interaction of different PS lines. As a result, straight lines are replaced by vortex rivers which become broader and have finite curvature (Fig.2(b)). The vortex rivers are comparable to the vortex self-organization discussed in [21] under different boundary conditions. Along one vortex river, few vortex-antivortex pairs are propagated. The kinetics is determined by the motion of these pairs along the rivers and finally by their annihilation. Importantly, the sample average of OP never reaches zero, contrarily to the case of the large field  $a > a_{c2}$ . The total number of vortices in the beginning of the process is larger than  $\frac{\phi}{\phi_0}$  (Fig.2(b)) which is also an indication of the growing importance of chaotic behavior in the dynamics. The values of  $\sqrt{\delta x^2}$  are also strongly enhanced, reaching  $2\pi R/3$ . The velocity of vortices along the rivers becomes smaller which is seen from the time dependence of the vortex number (Fig.2(d)). Nevertheless the velocity is still high compared to the case when the OP has recovered to its equilibrium value. The last regime  $a > a_{c2}$  is presented in Fig.2(c). Here the quench condition is satisfied and the OP decreases uniformly until it reaches zero (Fig. 2(c)). As a result, the new phase starts to grow uncorrelated and the vortices are created randomly. The number of vortices is substantially larger than  $\frac{\phi}{\phi_0}$ . Most of these vortices recombine rapidly. The remaining vortices move slowly through the sample propagating the  $2\pi$  phase jump. The random dispersion of these vortices is a fingerprint of the KZ mechanism. Indeed,  $\sqrt{\delta x^2}$  reaches now  $2\pi R/2$ , which means that vortex distribution is completely random. Another characteristic of the KZ scenario is that the vortices are created

while the order parameter is very close to zero and not during the fast growth like in the previous cases as one can see by comparing Fig. 2(a) and (b) with Fig. 2(c). It is important to notice that the total net vorticity is strictly equal to zero at any time in the case of periodic boundary condition in the  $z$  direction.

For vacuum boundary conditions [18] the kinetics is very similar. When  $a_{c1} < a < a_{c2}$  and  $\frac{\phi}{\phi_0} < 10$  one or more lines with reduced OP are formed. The difference is that the PS lines here have finite curvature, because they start to grow from the edges of the film and finally connect each other. Further increase of the flux, keeping  $a$  constant leads to the formation of flux rivers. The most important difference is that not all "rivers" necessarily connect two edges of the film. As a result some of them ended in the middle of the film, leading to the relatively small vorticity. These remaining vortices and antivortices propagate slowly to the edges of the film and kinetic is determined by the slow vortex motion. The dynamics when  $a > a_{c2}$  is governed by KZ mechanism, as in the previous case but the total net vorticity may be finite.

In the case of an inhomogeneous superconductor, the effective coherence length is now  $z$ -dependent  $\xi(z) = \xi/\sqrt{b(z)}$ . Therefore only the middle part of the ring may be unstable while the other parts of the film remain in the metastable state. The introduction of  $z$ -dependence of the parameters in Eq.(1) is designed to enhance the transverse vortex dynamics and allows to demonstrate different mechanisms of vortex formation. As expected, the PS dynamics starts first in the region with stronger current and is characterized by  $a$  and  $\frac{\phi}{\phi_0}$ .

In the region  $a_{c1} < a < a_{c2}$  and small flux  $\frac{\phi}{\phi_0} < 10$  the initial stage of the kinetics is similar to kinetics in the homogeneous film. The VaV pairs are not well defined. However, when kinematic VaV pairs approach the low current regions, they become well defined and are slowing down (fig.3(a)). Therefore vortices are stabilized near the line where the tangential velocity has discontinuity. These vortices represent another case of KH instability in

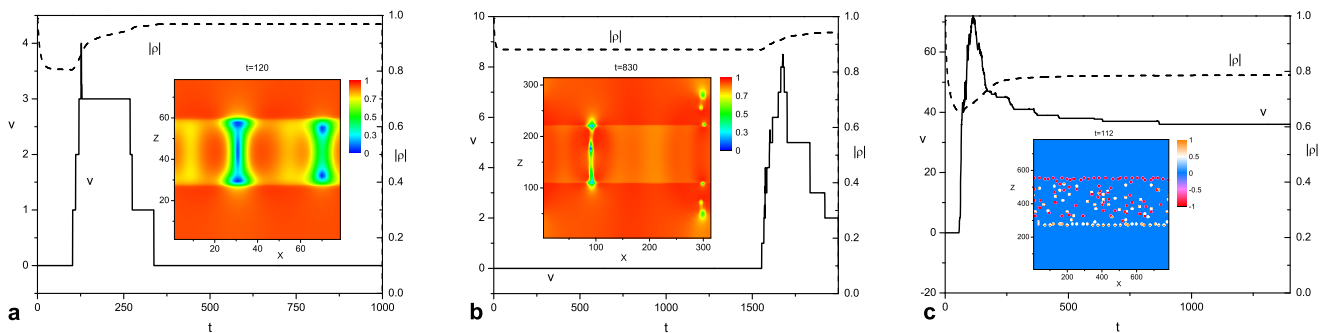


FIG. 3: (Color online) Total number of vortices  $v$  in the system and the sample average value  $|\rho|$  of the OP as a function of time for  $a_1 = 0.4$ ,  $\phi/\phi_0 = 5$  and  $b = 4$  (a);  $\phi/\phi_0 = 20$  and  $b = 2.25$  (b);  $\phi/\phi_0 = 50$  and  $b = 12.25$  (c). The insets represent snapshots of the amplitude of the OP at  $t = 120$  (a);  $t = 790$  and  $t = 830$  (b). For the quasi quenched case (c), the snapshot displays the local vorticity at  $t = 112$ .

superconductors. This instability leads to the formation of well defined vortices and governs the kinetics of the PS. To the best of our knowledge this is the only instability which allows vortex production in the low flux limit.

When the flux through the ring is large  $\frac{\phi}{\phi_0} > 10$ , the initial fast dynamics is similar to the dynamics in the homogeneous case until vortices reach the low current regions. Then they become slow and well defined. As it is seen in Fig.3(b), the vortices propagate one after another to the film edge, demonstrating the vortex-vortex attraction even in the case when the OP has already recovered.

The further increase of  $a > a_{c2}$  leads to the quench in the middle part of the film (Fig.1). During the quench many KZ vortices are created. Most of them are annihilated on a very short time scale. The rest reaches the line separating the region with different currents. The vortices almost stop near this line. The further dynamics is determined by the diffusion of these vortices to the film edges. When  $a$  is large enough, the KH vortices become well defined before the recovery of the OP in the middle part of the film and therefore the inhomogeneity suppresses the KZ mechanism in agreement with Ref.[14], making kinetics less stochastic.

Experimentally, observing such dynamics of vortices might be a real challenge because the short characteristic times does not allow the use of instruments with sufficient space resolution. However, recent works [11, 22] showed that freezing the dynamics can characterize both KZ and vortex river scenarios. Another idea is to use time resolved femtosecond optical spectroscopy as proposed in the Ref.[23]. As it is shown in the Refs.[4, 24] the role of heating is not important for the proposed geometry of the film.

We have considered the kinetics of the flux penetration to the 2D ring. We found out that for small values of the external field  $a$ , the kinetics is deterministic and essentially 1D. Increasing the flux  $\phi$  creates kinematic vortices and even leads to a 1D quench along the PS

line which is a first step towards stochastic behavior (see Ref.[24]). Further increase of  $a$  leads to the formation of vortex rivers, and ultimately to the quench of the sample leading to the stochastic dynamics of KZ vortices. The dynamics in the inhomogeneous film demonstrates that the VaV pairs are the topological analog of the PS mechanism in 2D but this analogy is not as straightforward as is often believed. Finally, our calculations for a partially quenched film indicate that KH vortices at the interface are strongly predominant.

- 
- [1] W.H. Zurek Physics Reports, **276**, 177 (1996).
  - [2] G.E. Volovik, Pisma ZhETF, **15**, 116 (1972).
  - [3] U. Parts *et al.*, Europhys. Letters, **31**, 449 (1995).
  - [4] M. Lu-Dac, V.V. Kabanov, Phys. Rev. B **79**, 184521 (2009); J. Phys.: Conf. Ser. **129**, 012050 (2008).
  - [5] A. Weber and L. Kramer, J. Low Temp. Phys. **84**, 289 (1991).
  - [6] A. Andronov *et al.*, Physica C **213**, 193 (1993).
  - [7] G.R. Berdiyrov *et al.*, Phys. Rev. B **79**, 184506 (2009).
  - [8] T.W.B. Kibble J. Phys. A, **9**, 1387 (1976).
  - [9] W.H. Zurek Nature, **317**, 505 (1985).
  - [10] V. M. Ruutu *et al.*, Nature **382**, 334 (1996); Phys. Rev. Lett. **80**, 1465 (1998).
  - [11] A. Maniv, E. Polturak, and G. Koren, Phys. Rev. Lett. **91**, 197001 (2003).
  - [12] T.W.B. Kibble, G. Volovik JETP Lett., **65**,102 (1997).
  - [13] N.B. Kopnin, E.V. Thuneberg, Phys. Rev. Lett., **83**, 116 (1999).
  - [14] I.S. Aranson, N.B. Kopnin and V.M. Vinokur, Phys. Rev. Lett., **83**, 2600 (1999).
  - [15] L.D. Landau, E.M. Lifshitz, Hydrodynamics. A.M. Fridman, Uspehi Fizicheskikh Nauk, **78**, 225 (2008).
  - [16] R. Blaauwgeers *et al.*, Phys. Rev. Lett. **89**, 155301 (2002)
  - [17] G.E. Volovik, Pis'ma ZhETF, **75**, 491 (2002). S.E. Korshunov, *ibid*, 496 (2002).
  - [18] P. G. de Gennes, *Superconductivity of Metals and Alloys* (Benjamin, New York, 1966).
  - [19] P. Laguna, W.H. Zurek, Phys. Rev. D, **58**, 085021, (1998).

- [20] D. Y. Vodolazov and F. M. Peeters, Phys. Rev. B **76**, 014521 (2007).
- [21] I. Aranson, B. Ya Shapiro and V. Vinokur, Phys. Rev. Lett. **76**, 142 (1996)
- [22] A. V. Silhanek *et al.*, Phys. Rev. Lett. **104**, 017001 (2010)
- [23] R. Yusupov *et. al.* arXiv:1006.1815, (2010).
- [24] Supplementary materials.

# Supplementary material for "Phase slip phenomena in superconductors: from ordered to chaotic dynamics"

Mathieu Lu-Dac and V. V. Kabanov  
*Jozef Stefan Institute, Jamova 39, 1001 Ljubljana, Slovenia*

## PHASE DIAGRAM OF THE DIFFERENT DYNAMICS

We observe different dynamics in the homogeneous case, depending on the value of the magnetic vector potential  $a$  and the number of flux quanta  $\phi/\phi_0$  penetrating the cylinder. In order to plot a phase diagram and display the different types of dynamics, we needed to choose between multiple criteria. We found out that the stochasticity is a good approach to this problem and chose the standard deviation of the  $x$  coordinate of vortices to define regions where the dynamics are comparable. The normalized standard deviation  $\frac{\sqrt{\delta x^2}}{\pi R}$  is shown in Fig.1 (R is the radius of the cylinder). The different regions where the standard deviation is similar are separated by lines of constant standard derivation.

- Part 1 of the phase diagram corresponds to the phase slip (PS) line solution. No vortices are present and we define there  $\frac{\sqrt{\delta x^2}}{\pi R} = 0$  because the dynamics is very ordered.
- Part 2 ( $0 < \frac{\sqrt{\delta x^2}}{\pi R} \leq 0.23$ ) corresponds to kinematic vortices traveling on a single line.
- Part 3 ( $0.23 < \frac{\sqrt{\delta x^2}}{\pi R} < 0.48$ ) is assigned to multiple vortex rivers : stochasticity is increased by the the increasing number of rivers.
- Part 4 ( $0.55 < \frac{\sqrt{\delta x^2}}{\pi R}$ ) corresponds to Kibble-Zurek (KZ) type dynamics which displays the highest possible stochasticity.
- Part 5 ( $0.48 < \frac{\sqrt{\delta x^2}}{\pi R} \leq 0.55$ ) represents the region where the standard deviation fails to clearly distinguish between KZ and vortex rivers. In this region, the area with low  $a$  corresponds to vortex rivers and should belong to the part 3. Indeed, when the flux is increased at low  $a$ , the number of vortex river increases and the vortices often travel from one river to the other : their position becomes stochastic. On the opposite, at low flux, the area with high  $a$  should belong to part 4.

## HEATING

The estimate of the heating of the cylinder may be done using Ohm's law. We consider that a part of the

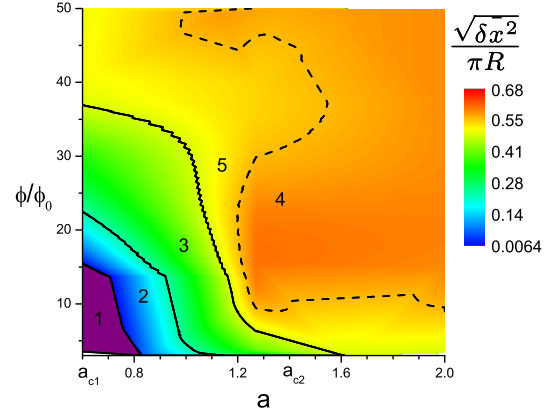


FIG. 1: (Color online) Phase diagram of the possible evolution drawn from the normalized standard deviation  $\frac{\sqrt{\delta x^2}}{\pi R}$  of the  $x$  coordinate of the vortices. We chose to define  $\frac{\sqrt{\delta x^2}}{\pi R} = 0$  when no vortices are present (Part 1). Part 1 corresponds to the PS line, part 2 the kinematic vortices, part 3 to vortex rivers and part 4 to KZ type dynamics. The part 5 represents a region where the standard deviation is not sufficient to distinguish between the dynamics. The standard deviation is plotted as a function of the vector potential  $a$  and of the number of flux quanta ( $a$ ) for  $u = 10$ .  $a_{c1}$  is the critical value under which dynamics are very improbable and  $a_{c2}$  is the critical value over which we calculated KZ dynamics would occur.

cylinder of area  $\pi\xi^2$  for the vortex or  $2\pi R\xi$  for the PS line, behaves like a normal conductor of conductivity  $\sigma_n$  until its annihilation and sustains a current  $J_s$  (in cgs units). The energy dissipated per unit of volume is, as in [1]:

$$E = \frac{J_s^2}{\sigma_n} \tau_\theta = \frac{[\phi_0 a(1 - a^2)]^2}{16\pi^3 \xi^2 \lambda_{\text{eff}}^2}. \quad (1)$$

This energy is less than a quarter of the condensation energy  $\frac{H_{c2}^2}{16\pi\kappa^2}$ . In the case of PS lines and kinematic vortices, when dynamics are fast and the areas behaving as normal conductors are small, the heat will be dissipated along the sample and through the contacts. It will not impact the dynamics. However, in the case of multiple vortex rivers or in the quenched KZ scenario, the total heating will be much larger but can be tackled by modern experimental techniques. Indeed, modern cooling methods are fast enough [2].

- 
- [1] M. Lu-Dac, V.V. Kabanov, Phys. Rev. B **79**, 184521 (2009); J. Phys.: Conf. Ser. **129**, 012050 (2008).
- [2] A. Maniv, E. Polturak, and G. Koren, Phys. Rev. Lett. **91**, 197001 (2003).